

Dynamics and Spectral Weights of Shake-up Valence Excitations in Resonant Inelastic X-ray Scattering

K. H. Ahn¹, A. J. Fedro^{1,2}, and Michel van Veenendaal^{1,2}

¹ Advanced Photon Source, Argonne National Laboratory,
9700 South Cass Avenue, Argonne, Illinois 60439

² Dept. of Physics, Northern Illinois University, De Kalb, Illinois 60115

(Dated: May 23, 2019)

We discuss the trends in the creation of valence excitations resulting from the screening of the core hole in resonant inelastic x-ray scattering (RIXS) for metals, semiconductors, and strongly correlated systems. We find that the inelastic spectral weight is not determined by the total energy of the shake-up structure, as is expected from simple considerations, but by the excitonic nature of the core hole and the valence electrons. The asymmetry between electron and hole excitations is emphasized and shown to be important in explaining the RIXS spectrum at, e.g., transition-metal K edges.

PACS numbers: 78.70.Ck, 71.20.-b, 61.10.Dp

The inelastic X-ray scattering cross section from a solid-state system can be enhanced by orders of magnitude, when the incoming x-ray energy ω_{in} is tuned to a resonance of the system which excites an electron from a deep-lying core state into the valence shell[1]. This is known as Resonant Inelastic X-ray Scattering (RIXS). In particular, for RIXS at transition-metal K edges, which has drawn significant attention recently[2, 3, 4, 5, 6, 7, 8, 9, 10], this involves a dipolar transition from the 1s shell into the wide 4p band. By studying the momentum, energy, and polarization dependence of the outgoing x-ray with energy ω_{out} and momentum q_{out} resulting from the radiative decay of the core hole, one can measure elementary excitations near the Fermi level or across the gap with an energy $\omega = \omega_{in} - \omega_{out}$ and momentum $q = q_{in} - q_{out}$. RIXS has several advantages compared to other spectroscopic probes. In contrast to angle-resolved photoemission, RIXS is bulk sensitive due to the large penetration depth of x-rays. The use of a particular resonance makes RIXS chemically selective, however, as opposed to x-ray absorption, there is no core hole present in the final state. RIXS has provided unique insights into, e.g., the momentum dispersion of charge excitations in high- T_c superconductors and related systems[3, 4, 5, 6, 7], orbital excitations[8, 9], and magnetic ordering dependent transfer of spectral weight in colossal magnetoresistive manganites[10].

The RIXS cross section is generally well described by the Kramers-Kramers-Heisenberg equation

$$I_{q_{in}q_{out}}(\omega_{in};\omega_{out}) = \sum_f \frac{1}{f} \int d\mathbf{r} G(\omega_{in}) T \frac{g_i g_f}{\omega_{in} - \omega_{out} - E_f};$$

where g_i and g_f are the ground and final states, respectively; we have taken the ground state energy $E_g = 0$; $T = A$ and $G(\omega) = (\omega_{in} - H + i\Gamma)^{-1}$, where H is the Hamiltonian of the system and the intermediate state lifetime broadening. It is important to realize that the spectral weights not only result from the transition operator T , but also from the screening dynamics due to the Coulomb interaction between the core hole

and the valence shell in the intermediate state[11, 12]. For K-edge RIXS, the attractive potential between the core hole and the 3d electrons is $U_c = 4-7$ eV. The interaction between the core hole and the excited 4p electron is small, and the 4p electron is mainly a delocalized spectator[13, 14, 15]. Therefore, the dipolar excitation effectively creates an unscreened core hole and charge flows in from neighboring ligands and transition-metals to screen the local core-hole potential. After the radiative 4p \rightarrow 1s deexcitation, the system is left with an intersite charge excitation due to the screening dynamics. Numerical calculations of the RIXS spectrum have been done on, e.g., finite clusters[3, 14]. Attempts have been made to relate RIXS to the dynamical structure factor $S_q(\omega)$, either by lowest-order perturbation theory[4, 7] or by an approximate representation of the intermediate state dynamics[15]. It was proposed that the probability for the intermediate state core-hole potential to create excitations, such as electron-hole pairs, mainly depends on the total energy of the shake up. In this Letter, we show that the RIXS strongly depends on the energies of the constituents of the excitation, leading to a strong asymmetry in electron and hole response to the core hole. We demonstrate that the RIXS spectral line shape is determined by the nature of the intermediate-state core hole-valence shell excitons.

In RIXS, excitations in the 3d derived valence states occur as a result of the strong core-hole potential in the intermediate state, $H_c = U_c \sum_i \frac{1}{r_i} \sum_i \frac{1}{r_i} \sum_i \frac{1}{r_i} \sum_i \frac{1}{r_i}$. We neglect the exchange term in the Coulomb interaction; $\frac{1}{r_i}$ and $\frac{1}{r_i}$ create a core hole and a valence electron at site i , respectively; $\sigma = \pm \frac{1}{2}$ is the spin of the 1s state and σ denotes the 3d spin and orbital degrees of freedom. Since the local core-hole potential does not introduce momentum selection rules, we are mainly interested in the energy dependence of the excitation process. We shall therefore study the angle-integrated RIXS. Since the 4p electron is treated as a spectator, we can write $T G(\omega_{in}) T = (z - H_d - H_c)^{-1}$, with $z = \omega_{in} - E_{1s,4p} + i\Gamma = 2$, where $E_{1s,4p}$ is the energy

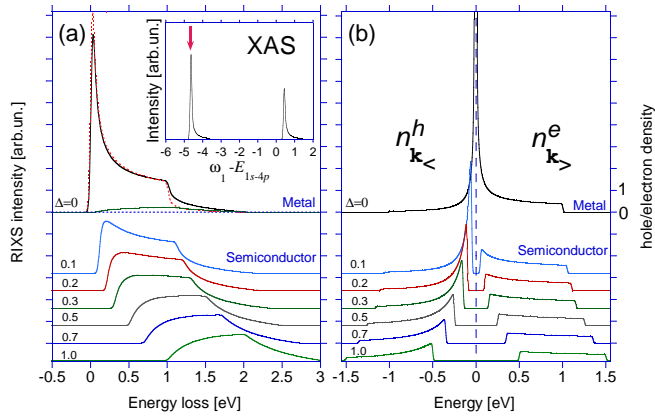


FIG. 1: (color) (a) Calculated R IX S spectra for a square density of states with band width $W = 2$ eV and $U_c = 5$ eV at half filling (black line, $\gamma = 0$ eV). For the semiconductors ($\Delta > 0$), a gap is opened at the center of the band. The inset shows the X-ray absorption spectrum (XAS) for $\gamma = 0$ eV. For them $\Delta = 0$, the green line shows the contribution of the double electron-hole pairs to the R IX S spectrum and the red dotted line gives the approximate spectrum using Eq. (1). (b) The intermediate state core-hole potential creates occupation of holes ($n_{k<}^h$) and electrons ($n_{k>}^e$) below and above the Fermi level, respectively, shown for different values of Δ .

necessary to make an excitation from the 1s to the 4p shell and H_d is the Hamiltonian describing the 3d-related electronic structure.

R IX S measures effectively the response of the valence system to a transient local potential $H_c = \frac{U_c}{N} \sum_{k \in \Gamma} d_k^{\dagger} d_k$, where N is the number of sites. Let us first consider the situation of independent particles with a single orbital degree of freedom, where $H_d = \sum_k \epsilon_k d_k^{\dagger} d_k$. In order to study how the core-hole potential produces inelastic spectral weight in metallic and semiconducting materials, we consider a simplified system of a square density of states (DOS) at half filling. To obtain a semiconductor the DOS is split at the Fermi level by a gap with size Δ . The neglect of electron-electron interaction in the valence shell allows us to treat the different spin channels separately.

The ground state is the Fermi sea given by $\langle j | j \rangle = \sum_k d_k^{\dagger} j | j \rangle$, where $j | j \rangle$ is the vacuum state and the product goes over the $L = N = 2$ occupied states. For the intermediate state, a DOS perturbed by a local potential is an exactly-solvable one-particle problem, whose solutions are given by the Green's function $[(\sum_k G_k^0(z))^{-1} + U_c]^{-1}$ with the unperturbed Green's function $G_k^0(z) = (z - \epsilon_k)^{-1}$. Taking the N eigenenergies E_m ordered, $E_1 < E_2 < \dots < E_N$, the lowest intermediate state can be written as $j_{\text{low}} | j \rangle = \sum_{m=1}^L d_m^{\dagger} j | j \rangle$, where d_m^{\dagger} creates an electron in the eigenstate with energy E_m .

The inset in Fig. 1(a) shows that the X-ray absorption spectrum (XAS) with two distinct spectral bands which correspond to valence states with an almost full or almost empty bound state. For the lower spectral band, the XAS spectral weight is dominated by the transitions

into $j_{\text{low}} | j \rangle$, whereas higher lying states in this band become rapidly orthogonal to the ground state. In our calculation, we focus on the situation where the incoming photon energy ω_{in} is tuned to the lowest intermediate state, which is a typical situation for momentum and energy resolved R IX S experiments. To obtain the R IX S spectral line shape, we study the decay of $j_{\text{low}} | j \rangle$ into the different final states. For the evaluation of the many-body matrix elements, we make use of the method described by Feldkamp and Davis [16]. For clarity, we omit the elastic contribution from our spectral line shapes and focus on the inelastic final states. For the creation of an electron-hole pair, we have configurations of the type $j_{\text{high}} | j \rangle = d_{k<}^{\dagger} d_{k>} | j \rangle$, where $k<$ and $k>$ represent states below and above the Fermi level, respectively. Since for a particular ω_{in} , the matrix element for absorption $j_{\text{low}} | j \rangle$ is equal for all R IX S final states, the R IX S spectral weights are proportional to $| j_{\text{high}} | j_{\text{low}} | j \rangle|^2$. It is straightforward to extend this procedure to higher numbers of electron-hole pairs. Our calculations show that the contribution of double electron-hole pairs is of the order of a few percent, see the green line in Fig. 1(a), whereas higher electron-hole pairs have a negligible contribution to the R IX S spectral line shape.

The results in Fig. 1(a), for a band width of $W = 2$ eV and a core hole potential of $U_c = 5$ eV, differ significantly from the existing approaches in Ref. [4, 7, 15] that predict that the on-resonance R IX S spectral line shape is proportional to the dynamical structure factor $S(\omega)$, i.e., the convolution of the occupied and the unoccupied DOS, weighted by the energy of the shake-up structure. For a square DOS, the R IX S on resonance is given by $S(\omega)$, which has a triangular shape, multiplied by a $U^2 = \omega^2$ [4, 7] or a $U^2 = (U - \omega)^2$ [15] energy dependence. However, Figure 1 clearly shows strong deviations from a simple triangular line shape. For the metallic system ($\Delta = 0$), we see a strong singularity close to zero energy loss related to the X-ray edge singularities [17]. In R IX S, however, the edge singularity is largely obscured by the presence of a large elastic peak and one is more interested in the high energy component of the spectral line shape. For higher energies, we find R IX S intensity up to 1 eV, i.e. half of the band width. At energies larger than 1 eV, the intensity quickly decreases to zero. For a small semiconducting gap, the singularity disappears and the R IX S spectral line shape resembles more closely the unoccupied DOS than $S(\omega)$. For larger gap values of the order of the band width, the spectral line shape develops into a triangular shape. The key to understanding the R IX S spectral line shape lies not in the total energy of the shake-up structure, but in understanding the nature of the excitonic states of the core hole and the valence shell in the intermediate state, leading to electron density above and hole density below the Fermi level. From the unitary transformation between the eigenstates with and without core hole $d_m^{\dagger} = \sum_k a_{m,k} d_k^{\dagger}$ with $a_{m,k} = C_m (\epsilon_k - E_m)$, where C_m is a normalization factor, the electron and hole densities projected from the lowest intermediate state,

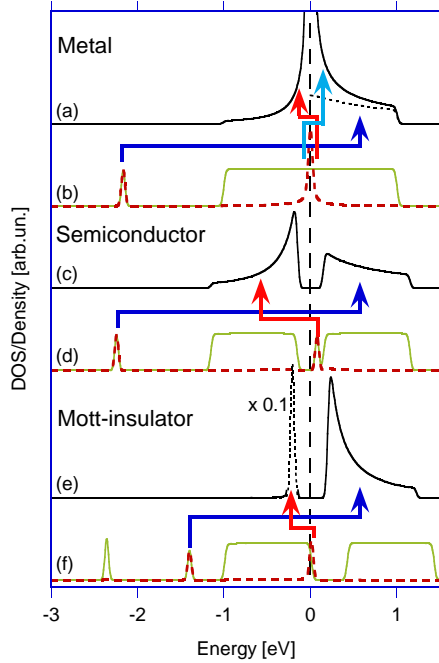


FIG. 2: (color) (a), (c), and (e) show the occupation of holes below the Fermi level and electrons above the Fermi level in the intermediate state for a metallic system, a semiconducting system ($\Gamma = 0.3$ eV), and a Hubbard system ($U = 1$ eV), respectively. For illustrative purposes a smaller core-hole potential ($U_c = 2$ eV) is chosen. The dotted line in 1(a) indicates the contribution of the excitonic bound state to the electron occupation above the Fermi level. The green solid lines in (b), (d), and (f) show the intermediate state densities of states for the metallic, semiconducting, and Hubbard systems, respectively. The red dashed lines and the arrows indicate how much the intermediate state density of states contributes to the electron densities above the Fermi level and hole densities below the Fermi level.

$n_{k>}^e = \sum_{m=1}^L a_{m k>}^2$ and $n_{k<}^h = \sum_{m=L+1}^N a_{m k<}^2$, can be calculated, as shown in Fig. 1(b). Although the RIXS spectral line shapes are calculated exactly, it is worthwhile to note that the RIXS spectrum is well described by the approximate expression

$$I(!) = A \sum_{k> k<} n_{k>}^e n_{k<}^h (1 - \delta_{k>} + \delta_{k<}); \quad (1)$$

with A a numerical factor, as shown with a red dotted line in Fig. 1(a). This approximation is valid as far as the final states are one electron-hole pair states and electron and hole wavefunctions are separable. Therefore much insight into the shape of $I(!)$ can be obtained from the understanding of $n_{k>}^e$ and $n_{k<}^h$. In the intermediate state, the strong core-hole potential pulls out a bound state with energy $E_b = E_1 = U_c - \frac{W^2}{12U_c}$ below the bottom of the band, see Fig. 2(b). This bound state contributes to the electron density above the Fermi level of the form $n_{k>}^{e_b} = \frac{1}{N} E_b^2 - \frac{W^2}{2} = (\delta_{k>} - E_b)^2$, shown as the dotted line in Fig. 2(a). The other eigenstates in the band are shifted [16] according to $E_m = \delta_{k_m} - \frac{mW}{N}$ for $m > 1$,

where, for large U_c values, the phase shift $\phi_m = \pi$ for $\delta_{k_m} = \frac{W}{2}, \dots, \frac{W}{2}$. The phase shift at the Fermi level $\phi_0 = \frac{\pi}{2} \arctan \frac{W}{U_c}$ leads to the creation of low-energy electron-hole pairs resulting in the edge singularity. Although distribution functions $n_{k>}^e$, $n_{k>}^{e_b}$, and $n_{k<}^h$ differ close to the Fermi level, their high-energy tails are described by $W \sin^2 \phi_0 = (N^2 f_k)^2$. The physical picture of the RIXS spectral line shape is as follows. The low energy loss features of $n_{k<}^h$, $n_{k>}^e$, and $I(!)$ are dominated by the X-ray edge singularity. Larger energy loss features occur since an electron is bound to the core hole in the intermediate state. After recombination of the 1s core hole with the excited 4p electron, this electron scatters into all the unoccupied states. Although hole excitations are created locally, holes are not bound to the core hole and therefore couple strongly to the DOS close the Fermi level. Since the hole density $n_{k<}^h$ is much closer to the Fermi energy, while the electron density $n_{k>}^e$ spans the whole empty band, the RIXS resembles more closely the unoccupied DOS. Note that when the energy is tuned to the satellite in the XAS spectrum, the situation is reversed. The exciton state is empty and the hole in the bound state scatters to all the occupied states.

The situation changes when a semiconducting gap is opened. The Fermi level now shifts to the center of the gap, and two bound states are formed, see Fig. 2(d), with energies $\frac{U_c}{2} \pm \frac{1}{2} \sqrt{U_c^2 + \frac{W^2}{4}}$ in the limit $U_c \ll W$. In the limit $U_c \gg W$, this gives one bound state below the bottom of the band at $E_b^e = -U_c$ and the other inside the gap at $E_b^h = 0$. Expressions for larger W are more complex, but give essentially the same physics. From Fig. 1(b) we see that the singularity disappears when the semiconducting gap increases. From Fig. 2(d), we clearly see that the electron density above the Fermi level and the hole density below the Fermi level originate predominantly from the bound states. Note, however, the strong asymmetry in the distribution below and above the Fermi level. The distribution functions are given by $n_{k>}^{e_b} = (\delta_{k>} - E_b^e)^2$. Note that the energy difference between the lowest bound state and the bottom of the conduction band is $U_c + \frac{W^2}{4}$, whereas the energy difference between the bound state inside the gap and the top of the valence band is only $\frac{W^2}{4}$. This stronger coupling of the bound state inside the gap with the valence band leads to the peaked nature of the hole distribution below the Fermi level.

The relationship between the RIXS spectrum and the dynamical structure factor is one of the interests of recent studies. Our results on the form of $n_{k<}^h$ and $n_{k>}^e$ allows us to find explicit expressions of $I(!)$ in certain limiting cases, which can be compared with $S(!)$. For example, in the limit $U_c \ll W$, we obtain that RIXS is proportional to $S(!) = [\frac{1}{2}(\delta_{k>} - \frac{W}{2})]$ and $S(!) = [\frac{W}{2}(\delta_{k>} - \frac{W}{2})]$, in the regions $|\delta_{k>}| < W$ and $W > 2$, where $S(!) = 0$ and $+W > |\delta_{k>}| + W$, where $S(!) = +W$, respectively. In this limit, we find that the integrated spectral weight approaches $A = \int_{k>} n_{k<}^h n_{k>}^e$ or $A = 4$ in the case

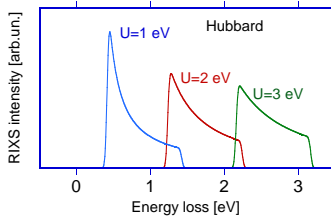


FIG. 3: (color) RIXS spectral line shapes resulting from tuning the incoming photon energy to the lowest intermediate state for on-site Coulomb interactions $U = 1, 2$, and 3 eV.

of half filling as a function of ϵ , recovering the limiting case found by Van den Brink and Van Veenendaal [15].

For independent particles with a single orbital degree of freedom, the other spin channel would be equivalent and one has two bound states on the site with the core hole in the intermediate state. However, for transition-metal compounds, the Coulomb interaction between valence electrons is often non-negligible. To study this, we consider the Hubbard model which has an additional on-site Coulomb term $U_{\sigma} d_{i\sigma}^{\dagger} d_{i\sigma} d_{i\sigma}^{\dagger} d_{i\sigma}$. The Hubbard model cannot be solved exactly, but the main features can be understood by following Hubbard's approach [18], which we use as a starting point of our analysis of the RIXS spectral line shape. The on-site Coulomb interaction splits the DOS into lower and upper Hubbard bands (LHB and UHB) with a gap proportional to U . With the two spin degrees of freedom on the site with the core hole, two bound states are pulled below the bottom of the LHB, see Fig. 2(f). The lowest bound state at approximately U_c below the LHB consists mainly of states from the LHB. The second bound state, which is about U higher in energy, has mainly UHB character. For the lowest intermediate state, both bound states are filled giving an energy of $2U_c + U$, which is equivalent to two electrons on a site with a core hole. After the de-excitation, these electrons can scatter to different states.

However, the states from LHB were already occupied in the ground state and do not contribute to the inelastic scattering, see Fig. 2(f). In contrast, in the ground state, very little doubly occupied states are present and the second bound state leads to scattering to all the states in the UHB. After filling the two bound states, we have $N-2$ electrons left to fill the $N-1$ states in the LHB in the intermediate state. For the lowest intermediate state, one therefore finds a hole at the top of the LHB and the hole scatters only to a narrow region of the occupied DOS, see 2(e) and 2(f). The RIXS spectral line shape therefore mainly reflects the unoccupied DOS as is clear from the RIXS spectra in Fig. 3 for $U = 1, 2$; and 3 eV, where the incoming photon energy is tuned to the lowest intermediate state. Note that the width of the RIXS spectrum is $W=2$, i.e. the width of the UHB. Tuning the photon energies to higher energies leads to a scanning of the LHB.

In summary, we have shown that the spectral weight of charge excitations in transition-metal K-edge RIXS, where the core-hole potential is larger than the effective bandwidth, is not determined by the total energy of the shake-up, but results mainly from the nature of the intermediate state core-hole-valence shell excitons. The strong difference in exciting electrons and holes make it difficult to interpret the spectral line shape in terms of S_q (!), obtained from, e.g. ab initio calculations, multiplied by a resonance function. However, the methodology described in this Letter can be straightforwardly extended to more complicated systems allowing a better interpretation of transition-metal K-edge RIXS.

We thank John Hill, Stephane Grenier, and Jeroen van den Brink for discussions. Work at Argonne National Laboratory was supported by the U.S. Department of Energy, Office of Basic Energy Sciences, under contract W-31-109-Eng-38. MvV was supported by the U.S. Department of Energy (DE-FG02-03ER46097) and the Laboratory for Nanoscience, Engineering, and Technology under a grant from the U.S. Department of Education.

[1] For a review, see A. K. Otani and S. Shin, *Rev. Mod. Phys.* 73, 203 (2001).

[2] C. Kao et al., *Phys. Rev. B* 54, 16361 (1996).

[3] J. P. Hill et al., *Phys. Rev. Lett.* 80, 4967 (1998).

[4] P. Abbamonte et al., *Phys. Rev. Lett.* 83, 860 (1999).

[5] M. Z. Hasan, et al., *Science* 288, 1811 (2000); M. Z. Hasan, et al., *Phys. Rev. Lett.* 88, 177403 (2002).

[6] Y.-J. Kim, et al., *Phys. Rev. Lett.* 89, 177003 (2002); Y.-J. Kim, et al., *ibid.* 92, 137402 (2004).

[7] G. Doring, et al., *Phys. Rev. B* 70, 085115 (2004).

[8] E. Saito, et al., *Nature* 410, 180 (2001).

[9] H. Kondo, S. Ishihara, and S. Maekawa, *Phys. Rev. B* 64, 014414 (2001).

[10] S. Grenier et al., cond-mat/0407326

[11] see, e.g. M. van Veenendaal and A. J. Fedro, *Phys. Rev. Lett.* 92, 219701 (2004).

[12] M. van Veenendaal and P. Carras, *Phys. Rev. Lett.* 78, 2839 (1997).

[13] K. T. Sutsui, T. Tohyama, and S. Maekawa, *Phys. Rev. Lett.* 83, 3705 (1999); *ibid.* 91, 117001 (2003).

[14] T. Nomura and J.-I. Igarashi, *J. Phys. Soc. Jpn.* 73, 1677 (2004), and cond-mat/0312624.

[15] J. van den Brink and M. van Veenendaal, cond-mat/0311446v1.

[16] L. C. D avis and L. A. Feldkamp, *J. Appl. Phys.* 50, 1944 (1979); L. A. Feldkamp and L. C. D avis, *Phys. Rev. B* 22, 4994 (1980).

[17] G. D. Mahan, *Phys. Rev.* 163, 612 (1967); P. Nozieres and C. T. De Dominicis, *ibid.* 178, 1097 (1969).

[18] J. Hubbard, *Proc. Roy. Soc. London Ser. A* 276, 238 (1963).